RESEARCH ARTICLE doi.org/10.1002/adsc.202100639

Advanced Synthesis & Catalysis

Very Important Publication

A Mechanistic Probe into 1,2-*cis* Glycoside Formation Catalyzed by Phenanthroline and Further Expansion of Scope

Jiayi Li[a] and Hien M. Nguyen[a,*]

[a] Department of Chemistry, Wayne State University, Detroit, Michigan, 48202, United States
E-mail: hmnguyen@wayne.edu

Manuscript received: May 25, 2021; Revised manuscript received: June 22, 2021;
Version of record online: ■■, ■■

Supporting information for this article is available on the WWW under https://doi.org/10.1002/adsc.202100639

Abstract: Phenanthroline, a rigid and planar compound with two fused pyridine rings, has been used as a powerful ligand for metals and a binding agent for DNA/RNA. We discovered that phenanthroline could be used as a nucleophilic catalyst to efficiently access high yielding and diastereoselective α-1,2-*cis* glycosides through the coupling of hydroxyl acceptors with α-glycosyl bromide donors. We have conducted an extensive investigation into the reaction mechanism, wherein the two glycosyl phenanthrolinium ion intermediates, a $^4C_1$ chair-liked β-conformer and a $B_{2,5}$ boat-like α-conformer, have been detected in a ratio of 2:1 (β:α) using variable temperature NMR experiments. Furthermore, NMR studies illustrate that a hydrogen bonding is formed between the second nitrogen atom of phenanthroline and the C1-anomeric hydrogen of sugar moiety to stabilize the phenanthrolinium ion intermediates. To obtain high α-1,2-*cis* stereoselectivity, a Curtin-Hammett scenario was proposed wherein interconversion of the $^4C_1$ chair-like β-conformer and $B_{2,5}$ boat-like α-conformer is more rapid than nucleophilic addition. Hydroxyl attack takes place from the α-face of the more reactive $^4C_1$ β-phenanthrolinium intermediate to give an α-anomeric product. The utility of the phenanthroline catalysis is expanded to sterically hindered hydroxyl nucleophiles and chemoselective coupling of an alkyl hydroxyl group in the presence of a free C1-hemiacetal. In addition, the phenanthroline-based catalyst has a pronounced effect on site-selective couplings of triol motifs and orthogonally activates the anomeric bromide leaving group over the anomeric fluoride and sulfide counterparts.

Keywords: Phenanthroline, NMR Study; Kinetics; 1,2-*cis* Glycosides; Stereo- and Site-Selective; Orthogonal Activation

Introduction

The field of glycoscience has burgeoned in the last decades, leading to the identification of glycans that play critical roles in a wide range of biological processes.[1] This rapid growth of knowledge about the function of glycans has attracted increasing attention from biological, pharmacological, and medicinal researchers. Meeting their research demands requires access to significant quantities of well-defined natural and unnatural glycans. Further, access to biologically relevant oligosaccharides and glycoconjugates enables the identification protein binding epitopes and provides standards for the development of analytical methodologies. This has prompted resurgence in synthetic interest, with a particular focus on new and robust approaches to the formation of α- or β-selective C–O bonds at the anomeric center.

Despite recent breakthroughs,[2] glycan synthesis remains a challenging endeavor because of the stereoselective installation of glycosidic C–O linkages. In particular, the identification of approaches to the coupling of hydroxyl acceptor (nucleophile) with sugar donor (electrophile) to form 1,2-*cis* glycosidic linkage in high yield and diastereoselectivity remains a major goal. Glycosylation strategies often rely on neighboring group participation, steric and electronic properties, and directing effects to influence 1,2-*cis* selectivity.[3] As a result, they remain substrate-dependent. In addition, subtle changes to carbohydrate structure or protecting groups have profound impacts on the glycosylation reactivity and selectivity.

The use of catalysts, which are consisted of enzymes, transition-metal complexes, or small organic molecules, has emerged as a promising strategy to address the challenges associated with carbohydrate synthesis.[4] Particularly, nucleophilic catalysts play a central role in expanding chemical space of small organic molecule catalysis and are capable of catalyzing a variety of organic transformations.[5,6] A wide range of Lewis bases, tertiary phosphines/amines, pyridines, and imidazoles, have been showed to act as effective, nucleophilic catalysts.[5] For instance, glycosylation reaction promoted by pyridine has been reported.[7] However, the pyridine-promoted reaction proceeds with marginal diastereoselectivity for α-1,2-*cis* glycoside due to the competing formation of β-1,2-*trans* glycoside.

We recently discovered that phenanthroline effectively catalyzed the glycosylation of a variety of alcohol nucleophiles with α-glycosyl bromides to provide α-1,2-*cis* glycosides with the net retention of the anomeric configuration (Scheme 1).[8] This phenanthroline catalysis system provides a general platform for predictable and stereoselective formation of 1,2-*cis* glycosidic linkages under mild and operationally simple conditions. As a result, a proper mechanistic understanding of phenanthroline-catalyzed glycosylation is critical for the development of robust α-1,2-*cis* glycoside procedure. Herein, we report the use of deuterated glucosyl bromide as a glycosyl donor and examined the stereochemical outcome of glycosylations with piperidine substituted phenanthroline catalyst. We unveiled the mask of the glycosyl phenanthrolinium ion intermediates using variable temperature NMR (^{1}H, COSY, and ROESY) experiments. Kinetic studies showed that the rate of glycosylation is dependent on the concentration of the phenanthroline catalyst, glycosyl donor, and acceptor. A detailed understanding of phenanthroline-catalyzed glycosylation mechanism has led to a broader scope. This phenanthroline catalyst system not only fulfills high α-1,2-*cis* diastereoselectivity, but also enables high chemo- and site-selectivity.

Results and Discussion

Phenanthroline has been utilized extensively as a powerful ligand for metals and a binding agent for DNA/RNA.[9] However, there was no report on the use of phananthroline as a nucleophilic catalyst in organic reactions or stereoselective glycosylations until our recent discovery.[8] Our initial proposed mechanism evolved from a basic principle: two pyridine nitrogen atoms are positioned to act cooperatively (Scheme 2). The first nitrogen atom acts as a catalytic nucleophile to displace the C1-anomeric bromide leaving group of a glycosyl donor, via an S_N2-like pathway, to generate an equatorial (β) phenanthrolinium ion intermediate preferentially to avoid the steric interactions associated with positioning that group in the axial (α) orientation. The second nitrogen atom could interact with carbohydrate moiety to further stabilize the phenanthrolinium ion intermediate. Subsequent S_N2-like substitution by a hydroxyl nucleophile leads to the formation of α-1,2-*cis* glycosides.

Detection of Glycosyl Phenanthrolinium Ion Intermediates. For the phenanthroline-catalyzed glycosylation to yield α-1,2-*cis* product, the catalyst must associate with either or both substrates in the reaction. In our proposed mechanism (Scheme 2), phenanthroline displaces the bromide leaving group to form a glycosyl phenanthrolinium ion intermediate. Unlike sugars, phenanthroline is a rigid and planar organic compound with a C_2 symmetry. However, if phenanthroline is coupled with a sugar molecule, the symmetry will be destroyed. As a result, our first objective was to perform ^{1}H NMR study to observe the symmetry on phenanthroline (Figure 1). To obtain a clear view on the aromatic region in ^{1}H NMR, 2,3,4,6-tetra-benzyl-d_7-glucopyranosyl bromide **1*** was used as an electrophile, wherein the chemical shift of anomeric proton (H_1) resonance appeared at $\delta_H =$ 6.55 ppm in CD_2Cl_2 (Figure 1a). Piperidine substituted phenanthroline **C2** was chosen for our NMR study because it is the most effective catalyst[10] compared to other catalysts,[8] implying formation of the reactive glycosyl intermediates is more favorable. In addition,

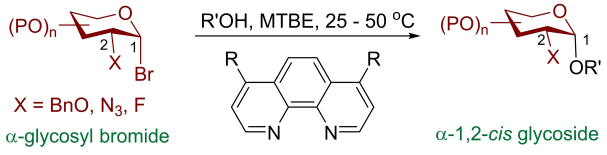

Scheme 1. Phenanthroline-catalyzed α-1,2-*cis* glycosylations

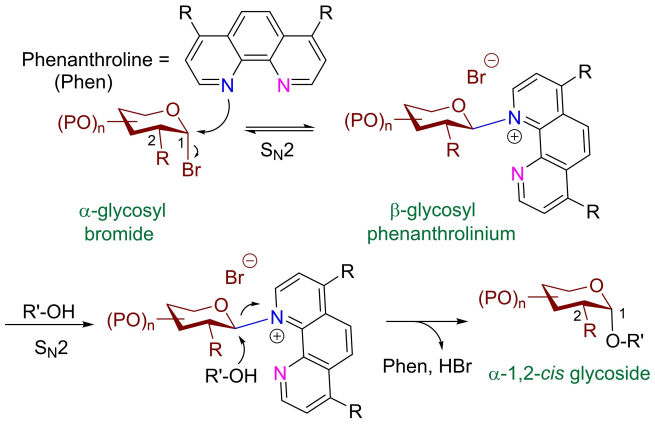

Scheme 2. Proposed mechanism of the phenanthroline-catalyzed α-1,2-*cis* glycosylations

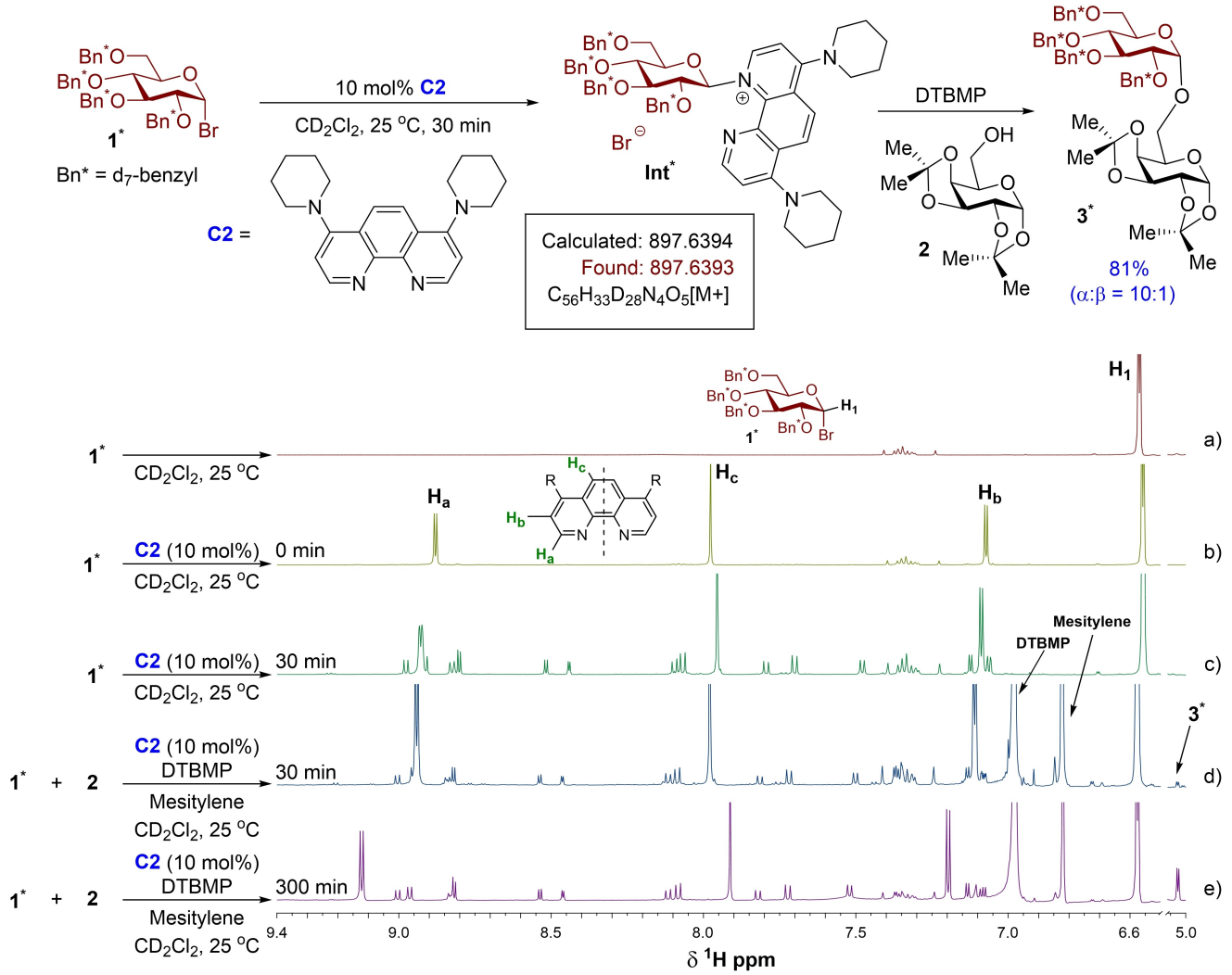

Figure 1. Detection of phenanthrolinium intermediate by ^{1}H NMR: (a) Deuterated *tetra*-benzyl glucosyl bromide **1*** in CD_2Cl_2; (b) **1*** and 10 mol% **C2** at 0 min; (c) **1*** and **C2** at 30 min, new signals emerging around phenanthroline aromatic region; (d) **1***, **2**, **C2** at 30 min, disaccharide **3*** emerging; and (e) **1***, **2**, **C2** at 300 min, more disaccharide **3*** formed in the reaction. See supporting information for full spectra.

the chemical shift of the piperidyl substituents would not appear in the aromatic region. To avoid any possible side reaction with by-product of isobutyl oxide (IBO),[10] di-*tert*-butylmethylpyridine (DTBMP) was chosen as the acid scavenger in the later NMR experiment (Figure 1).

Upon addition of 10 mol% of **C2** to the deuterated glycosyl bromide **1***, three new signals appeared at $\delta_H = 8.88$ ppm (H_a, d, $J = 5.0$ Hz) and $\delta_H = 7.07$ ppm (H_b, d, $J = 5.1$ Hz) and the singlet at $\delta_H = 7.98$ ppm (H_c) represented the symmetry of **C2** catalyst (Figure 1b). Within 30 min, new signals emerged around the phenanthroline region (Figure 1c). These new signals were not detected in the mixture of nucleophile **2** and **C2** (Figure S1). An aliquot of the reaction mixture was subjected to electrospray ionization (ESI) mass spectrometry and returned m/z ratio of 897.6393, confirming the presence of the intermediate **Int*** (Figure 1) which resembled a phenanthrolinium ion. Hydroxyl nucleophile **2** was subsequently added to the reaction mixture along with DTBMP and mesitylene (internal standard). After 30 min, new signals still surrounded the aromatic region (Figure 1d) along with the appearance of the disaccharide product whose anomeric proton appeared at $\delta_H = 5.03$ ppm (d, $J =$ 3.6 Hz, Figure 1d). At 5 h, more product was formed and the new peaks remained at the aromatic region (Figure 1e). The reaction mixture was allowed to stir overnight at 25 °C. The product **3*** was isolated in comparable yield (80%) and selectivity (α:β = 10:1) to that of disaccharide **3** (*vide infra*, Table 1, entry 4). Several key observations were obtained from this

NMR experiment: (1) the new signals appeared to be doublets, indicating the newly-formed phenanthroline species did not maintain their symmetry; (2) the number of signals suggests that there are two possible phenanthroline species (**Int$_1$** and **Int$_2$**) present in the solution (Figure 2); (3) the population of unbound phenanthroline **C2** and the two phenanthroline species (**Int$_1$** and **Int$_2$**) shifted from 76:14:10 (**C2**: **Int$_1$**: **Int$_2$**) to 81:12:7 upon addition of alcohol **2**, suggesting the equilibrium of the catalyst states had shifted toward regeneration of **C2**, likely through formation of the coupling product; and (4) the integration of the signals suggested that an extra hydrogen atom appeared on the phenanthroline aromatic region for each newly-formed species, which was subsequently identified as a C1-proton of the sugar unit (*vide infra*, Figure 2).

To further identify the presence of the two newly-formed species upon mixing deuterated glycosyl bromide **1*** with **C2**, a 1:1 stoichiometry ratio of **1*** and **C2** catalyst was employed. As the concentration of **C2** increased, the equilibrium shifted toward the two new intermediates, wherein the population of unbound **C2** catalyst, **Int$_1$** and **Int$_2$** became 55%, 30%, and 15%, respectively (see SI for ^{1}H NMR spectrum). Variable temperature ^{1}H, ^{1}H-^{1}H 2D COSY and ROESY NMR spectra at 0 °C were subsequently obtained. Density functional theory (DFT) calculations were employed to assist the deconvolution of these intermediates. The geometries of possible intermediates' structures were optimized and vibrational frequencies were calculated at the B3LYP/6-31+G(d,p) level[11] with the SMD implicit solvent model[12] and the GD3BJ empirical dispersion correction[13]. All calculations were carried out with Gaussian 09.[14] In our DFT calculations, tetramethyl glucosyl bromide was used as a model electrophile to reduce computational cost (Figure 2). The DFT calculation results are consistent with our NMR data.

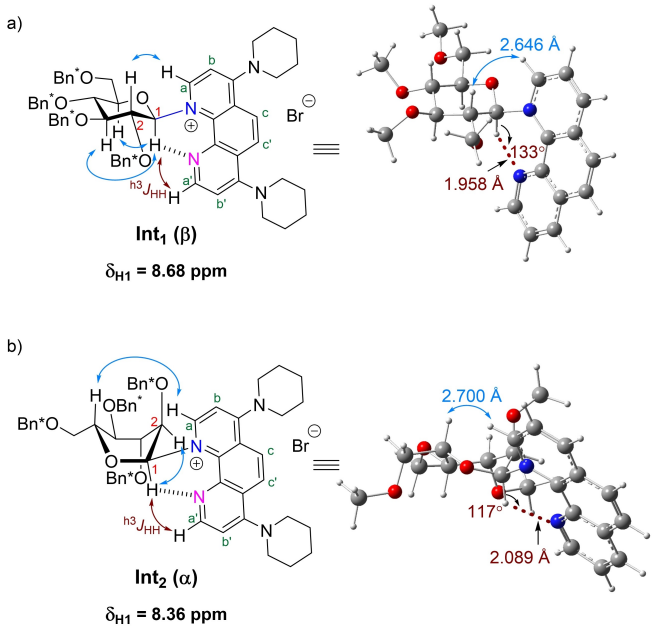

Figure 2. Conformation of the glycosyl phenanthrolinium ion intermediates: ^{1}H-^{1}H 2D COSY (red) and ROESY (blue) NMR evidence (see Figure S2 for correlations) as well as DFT calculation structures.

Employing 2D COSY NMR, the newly formed protons in the phenanthroline aromatic region resided at $\delta_H = 8.68$ ppm (d, $J = 8.1$ Hz) and $\delta_H = 8.36$ ppm (d, $J = 3.6$ Hz) were identified to be the C1 protons of the anomeric mixture of **Int$_1$** (β) and **Int$_2$** (α), in a ratio of 2:1 (β:α) (Figure 2). Suggested by DFT calculations (Figure 2), while H_a proton on the phenanthroline is spatially closed to the C2 proton for the β-isomer **Int$_1$** (2.646 Å), the H_a proton for the α-isomer **Int$_2$** is closed to the C5 proton (2.700 Å) on the sugar ring. These spatial interactions were also observed through 2D ROESY NMR, which consolidate the anomeric configurations for the two detected intermediates. Similar to the glycosyl pyridinium ion,[7,15] the major phenanthrolinium ion intermediate is a β-configured isomer (**Int$_1$**) and exists in the $^4C_1$ chair conformation while the minor α-isomer (**Int$_2$**) exists in the $B_{2,5}$ boat conformation to avoid stereo- and electronic effect from the ring.

Hydrogen Bonding in the Phenanthrolinium Ion Intermediates. Several NMR evidences were found below to support hydrogen bonding (H-bonding) interaction between the second nitrogen of phenanthroline and the C1 anomeric proton. In general, for H-bonding involving an electronegative acceptor such as oxygen or nitrogen, the donor nucleus experiences a deshielding effect.[16] Conversely, if the C1 anomeric proton is hydrogen bonding to the second nitrogen of phenanthroline, the chemical shift should appear more downfield in the ^{1}H NMR. It has been reported that the anomeric proton of β-glucosyl pyridinium bromide resonances at $\delta_H = 6.10$ ppm in D_2O.[17] In addition, Gin and coworker established anomeric mixture of glycosyl pyridinium species, wherein the anomeric protons resonance at $\delta_H = 6.63$ and 6.49 ppm in CD_2Cl_2 at −60 °C.[18] However, the ^{1}H NMR spectra of a 1:1 mixture of glycosyl bromide **1*** and **C2** taken at −60 °C (see Figure S3) showed the anomeric protons of the intermediates, **Int$_1$** (β) and **Int$_2$** (α), resonance at $\delta_H = 8.44$ and 8.18 ppm, respectively (Figure 2). The downfield shift of the anomeric protons of glycosyl phenanthrolinium ion intermediates compare to that of the reported glycosyl pyridinium species is likely due to an intramolecular hydrogen bonding between the anomeric proton and second nitrogen on phenanthroline.

A more direct hydrogen bonding observation is through hydrogen bond scalar coupling.[16] The scalar interaction arises from electron cloud between nuclei,

such as covalent bonds. Upon formation of H-bonding, the redistribution of electron density of the nuclei associate with H-bonding allows us to observe the scalar coupling using COSY experiment.[16] As shown in Figure 2, scalar couplings ($^{h3}J_{HH}$) between the anomeric proton and $H_{a'}$ on the phenanthroline were observed for both intermediates **Int$_1$** and **Int$_2$**. These scalar interactions mediated by the lone pair electrons on the second pyridine nitrogen of phenanthroline and the conjugated system are evidential for H-bonding between the anomeric proton and the second nitrogen of phenanthroline. In order to obtain a clear view of the hydrogen bond coupling in ^{1}H NMR, a rigid H-bonding network is required.[19] As hydrogen bond formation is highly dependent on temperature,[20] we cooled the 1:1 mixture of glucosyl bromide **1*** and **C2** in CD_2Cl_2 to −60 °C and gradually warm to room temperature. The ^{1}H NMR spectra were taken at 10 °C interval and combined (Figure S3a). The ^{1}H NMR spectrum was at highest resolution at −10 °C. The C1-anomeric proton of **Int$_1$** (β) showed a defined allylic splitting at −10 °C (see Figure S3b). Further, DFT optimized structures (Figure 2) for anomeric mixtures of the phenanthrolinium intermediates are consistent with the NMR observation: for **Int$_1$** (β) the H1–N' distance is 1.958 Å and the C1–H1–N angle is 133°, while those for **Int$_2$** (α) are 2.089 Å and 117°.

Proposed Mechanism. Based on the NMR study and DFT calculations,[10] a proposed mechanism for the phenanthroline-catalyzed α-1,2-*cis* glycosylation is illustrated in Figure 3. We hypothesize that the first pyridine nitrogen atom of the phenanthroline catalyst **C2** displaces the anomeric α-bromide leaving group of glycosyl donor to form the β-phenanthrolinium ion intermediate. This phenanthrolinium ion positions equatorially to avoid the steric and electrostatic interactions. Our recent DFT calculations suggest that formation of the β-covalent phenanthrolinium ion intermediate is reversible.[10] The β-covalent glycosyl intermediate adopts the $^4C_1$ chair conformation and is in equilibrium with the α-glycosyl intermediate whose exists in the $B_{2,5}$ boat conformation. Our NMR study showed that these two key intermediates, a major $^4C_1$ β-phenanthrolinium ion conformer (**Int$_1$**) and a minor $B_{2,5}$ α-phenanthrolinium ion conformer (**Int$_2$**) were formed in the reaction (Figure 2). To obtain high levels of diastereoselectivity, a Curtin-Hammett situation must be established: interconversion of the $^4C_1$ chair-like β-conformer and $B_{2,5}$ boat-like α-conformer via an oxocarbenium ion intermediate is rapid and much faster than the subsequent nucleophilic attack (Figure 3). In the NMR study, these two intermediates were formed and equilibrated within 30 min while the product formation typically required more than 1 h to

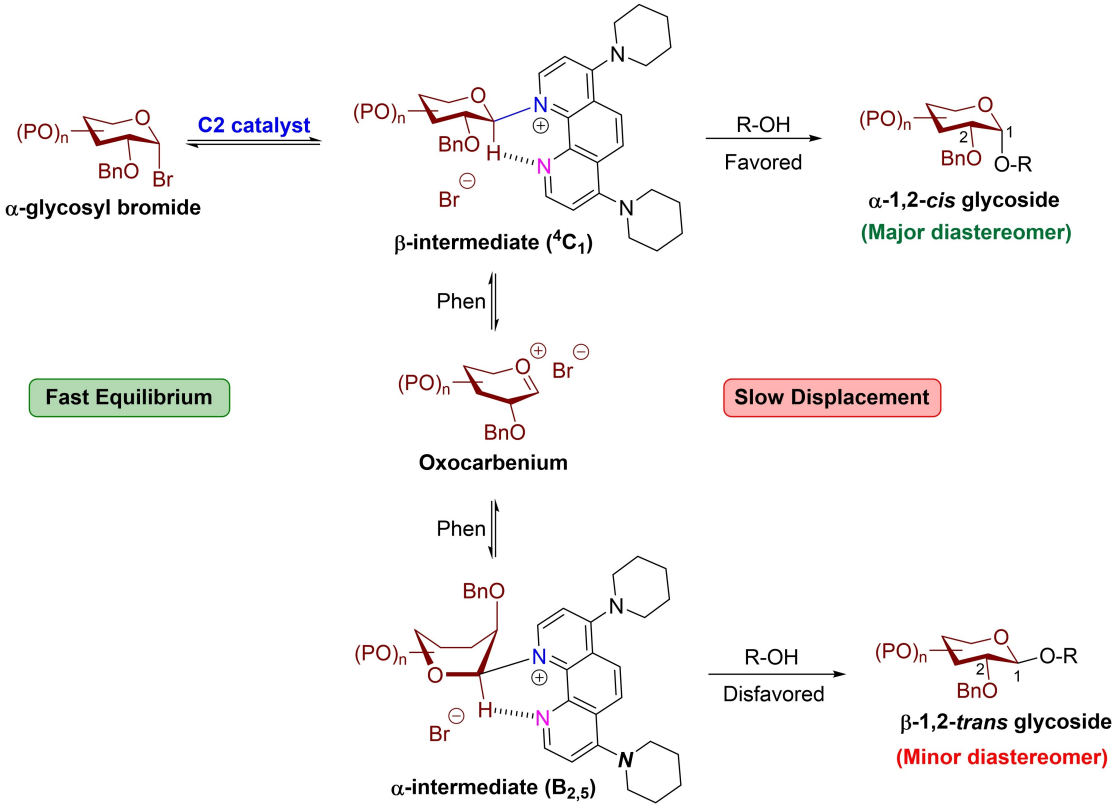

Figure 3. Possible mechanism of phenanthroline-catalyzed glycosylation

be observable. To rationalize the diastereoselectivity for the major α-1,2-*cis* product, hydroxyl acceptor preferentially approaches to the α-face of the $^4C_1$ chair conformation of the β-glycosyl phenanthrolinium ion intermediate via an S_N2 pathway. This would preclude the reaction proceeding through a disfavored $B_{2,5}$ boat conformation of the α intermediate, which leads to the minor β-1,2-*trans* product.

To further verify that the $^4C_1$ chair-like β-glycosyl phenanthrolinium is indeed the reactive intermediate, we sought to detect the intermediates for 2-deoxy-2-fluoro glycosyl bromide donor. The highly reactive tribenzyl 2-fluoro galactosyl bromide **4** was chosen as a model electrophile (Figure 4). The transient glycosyl phenanthrolinium ion intermediate (**Int$_3$**) was detected by ^{1}H NMR within several minutes (Figure 4) using a 1:1 mixture of 2-fluoro glycosyl bromide **4** and **C2** catalyst at 25 °C. Importantly, only the β-glycosyl phenanthrolinium ion intermediate **Int$_3$** (Figure 3) existing in the $^4C_1$ chair conformation was observed. In addition, more than 90% of **4** were converted to the **Int$_3$** intermediate within 2 h. Unlike the tetrabenzyl glycosyl bromide donor **1***, which produces highly interconvertible intermediates (**Int$_1$** and **Int$_2$**, Figure 2), the 2-fluoro galactosyl bromide **4** generates a more stable intermediate (**Int$_3$**), which results in either formation of the products or reverts to the reactant **4**. This observation was further supported by DFT calculations.[10]

The preferential formation of α-glucosides from α-glucosyl bromide in the presence of added bromide ion (Bu_4NBr) was first described by Lemieux and attributed to the enhanced reactivity of the higher energy β-glycosyl bromide.[21] As such, we evaluated if the stereochemistry of the α-1,2-*cis* product would be dictated by the configuration of glycosyl bromide at the anomeric carbon.[8] Because it is difficult to obtain β-isomer of glycosyl bromide in a pure form, a 5:1 mixture of β- and α-isomers of glycosyl bromide **5β/α** with β-isomer being a major diastereomer was used as a model substrate (Scheme 3).[8] We observed that a 5:1 β/α mixture of starting material **5β/α** slowly

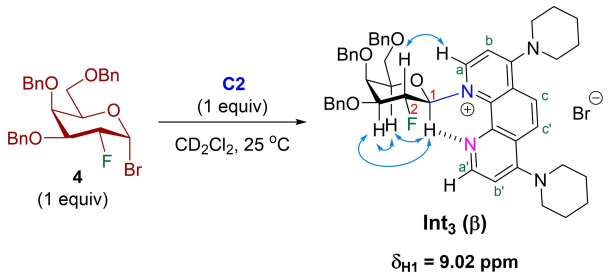

Figure 4. Conformation of the 2-deoxy-2-fluoro glycosyl phenanthrolinium ion and ROESY (blue) NMR evidence (see supporting information for full spectrum).

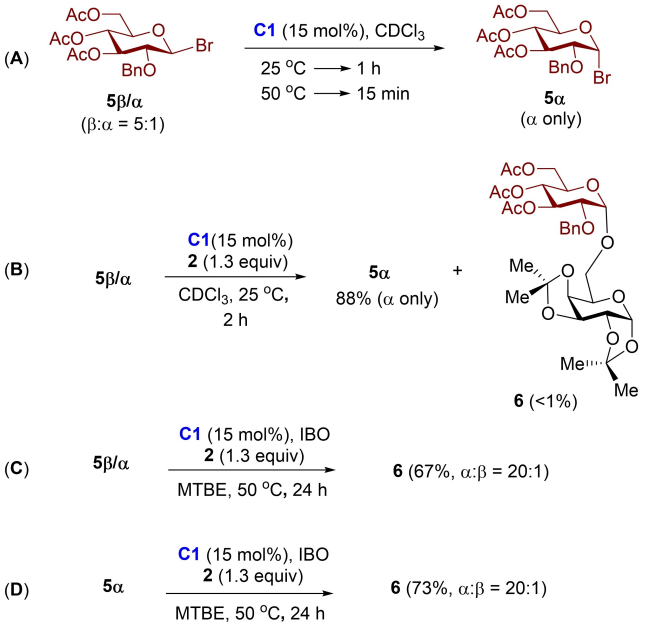

Scheme 3. Effect of the Configuration of Glycosyl Bromide

anomerized to the corresponding a 2:1 α/β mixture in the absence of the phenanthroline catalyst. However, a 5:1 β/α mixture **5β/α** converted exclusively to the corresponding α-isomer **5α** in the presence of 15 mol% of **C1** catalyst (*vide infra*, Table 1) within 1 h at 25 °C (Scheme 3A). We also performed the reaction of a 5:1 β/α mixture **5β/α** with galactoside acceptor **2** under the influence of **C1** catalyst at 25 °C. We observed isomerization of this 5:1 β/α mixture to α-isomer **5α** is faster than formation of the coupling product **6** at 25 °C (Scheme 3B). On the other hand, coupling of **2** with this 5:1 β/α mixture **5β/α** under standard **C1**-catalyzed conditions provided **6** (Scheme 3C) in comparable yield and α-selectivity to that obtained with α-isomer **5α** (Scheme 3D). Collectively, these results suggest that β-isomer of glycosyl bromide is not the reacting partner in the phenanthroline-catalyzed reaction. This catalysis, which derives its α-stereoselectivity from the highly reactive β-covalent phenanthrolinium ion intermediate, is different from the Lemieux system.[21]

Double S_N2 Mechanism? To further verify the glycosylation reaction undergoes double S_N2-like mechanism, we conducted kinetic investigation. Based on the NMR study, the rate of reaction is first order in the concentration of glycosyl bromide, hydroxyl, and catalyst. We reported the rate of phenanthroline **C1**-catalyzed glycosylation of 2-propanol with 3,4,6-tri-acetyl-2-*O*-benzyl-α-glucopyranosyl bromide **5α** is first-order in the concentration of alcohol and **C1** catalyst. In addition, the saturation behavior in 2-propanol concentration was observed.[8] However, due to solubility issue, we were not able to conduct the kinetic study with high concentration of glycosyl

bromide **5α**. In addition, we were not able to lower the glycosyl bromide concentration as the experiment required 60 h to obtain sufficient data under standard **C1**-catalyzed conditions.

To verify the glycosylation reaction is first-order dependent in the concentration of glycosyl bromide, we adapted the reagent system used in the NMR study and conducted kinetic experiment at varying glycosyl bromide concentration. The experiments were carried at 25 °C in CD_2Cl_2 with glucosyl bromide **1*** and **2** as the coupling partners, using **C2** catalyst, DTBMP, and mesitylene as internal standard. As illustrated in Figure 5a, the product concentration appeared linear relationship to time (apparent zero-order kinetics in substrates), and induction period was not observed. In addition, the rate of product formation increases as the concentration of glucosyl bromide **1*** increases. The initial rate of reaction in Figure 5b showed first-order dependence on glycosyl bromide **1***. Unfortunately, due to limiting amount of donor **1***, we were not able to observe the saturation behavior in glucosyl bromide concentration. However, the collective kinetic studies suggest that the phenanthroline catalyzed α-selective glycosylation undergoes associative mechanisms (likely double S_N2).

The rates of phenanthroline-catalyzed reactions with different substituents on the phenanthroline framework were also investigated. As illustrated in Figure 6, all three phenanthroline catalysts provide similar rate profile, where the overall rates are apparent zero-order kinetics in substrates and showing no induction period. Due to the electron donating effect of the piperidine substituents, the rate of **C2**-catalyzed glycosylation should be faster than that of **C1** and **C3** (*vide infra*, Table 1). As predicted, the **C2**-catalyzed reaction is more rapid than both **C1**- and **C3**-catalyzed reaction. On the other hand, both **C1** and **C3** showed similar rate, complementary to the observation in Table 1 (*vide infra*).

Influence of Phenanthroline To further validate the reaction outcome with the kinetic study (Figure 6), we first conducted the coupling of nucleophile **2** with undeuterated tetrabenzyl glucosyl bromide **1** in the presence of 15 mol% of **C1**, **C2**, and **C3** (Table 1). To distinguish the reactivity of different catalysts, we kept the reaction time for 5 h at 25 °C. Use of **C1** provided disaccharide **3** in 40% yield with α:β = 13:1 (entry 1). In contrast, use of **C2** provided **3** in higher high yield (67%, entry 3). The non-substituted phenanthroline **C3** yielded slightly less product compare to **C2** (67% vs. 40%, entry 5 vs. 3). These results are complementary to the kinetic experiment observed in Figure 6. As we observed in the NMR study, the C2-symmetry of phenanthroline plays critical role in the glycosylation. As such, we evaluated the mono-piperidine substituted phenanthroline **C4**, and a reduced yield of product **3** (24%, entry 7) was obtained in comparison to the symmetrical catalyst **C2** (entry 3), confirming the critical role of the symmetry on phenanthroline. Benzo [h]quinoline (**C5**, entry 8) catalyst is less reactive and α-stereoselective, further validating the hydrogen bond

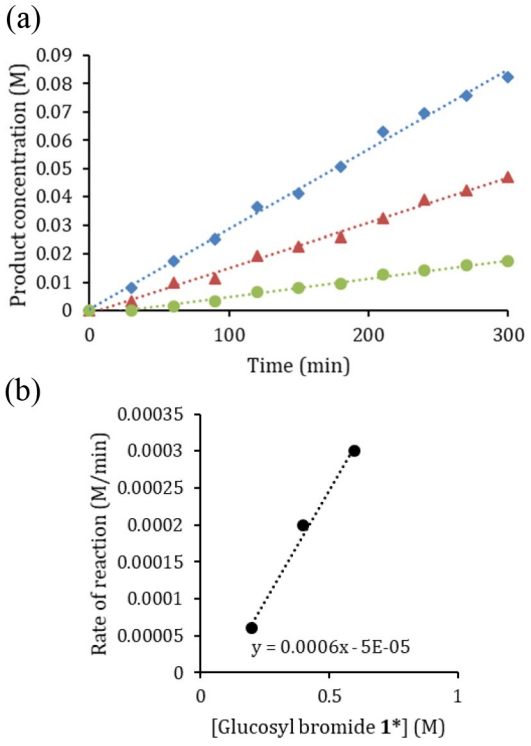

Figure 5. (a) Product concentration versus time for phenanthroline-catalyzed (**C2**, 0.02 M) glycosylation with varying glycosyl bromide concentration: 0.2 M **1*** (●, green), 0.4 M **1*** (▲, red) and 0.6 M **1*** (◆, blue). Reaction conditions: donor **1*** (0.2–0.6 M), acceptor **2** (0.2 M), **C2** (0.02 M), DTBMP (0.4 M), CD_2Cl_2 (5 mL), 25 °C; (b) the initial rate of reaction is dependent on the concentration of **1***.

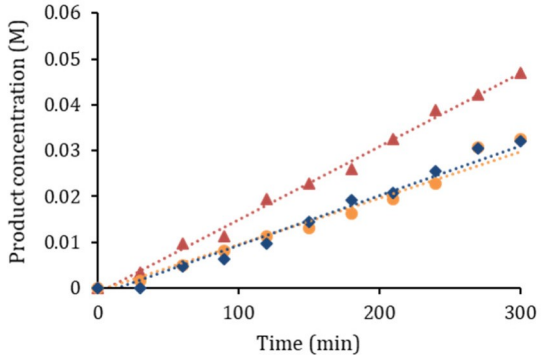

Figure 6. Product concentration versus time for the phenanthroline-catalyzed glycosylation with three different phenanthroline catalysts: **C1** (●, orange), **C2** (▲, red) and **C3** (◆, dark blue). Reaction condition: **1*** (0.4 M), **2** (0.2 M), catalyst (0.02 M), DTBMP (0.4 M), CD_2Cl_2 (5 mL), 25 °C.

Table 1. Influence of Phenanthroline-Based Catalysts[a]

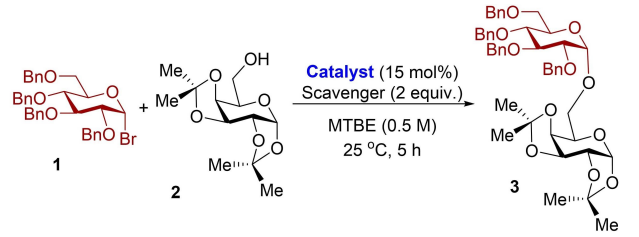

entry	Catalyst	Scavenger	yield[b] (α:β)[c]
1	**C1**	IBO	40% (13:1)
2	**C1**	DTBMP	31% (19:1)
3	**C2**	IBO	67% (12:1)
4	**C2**	DTBMP	63% (14:1)
5	**C3**	IBO	35% (14:1)
6	**C4**	IBO	24% (13:1)
7	**C5**	IBO	6% (5:1)

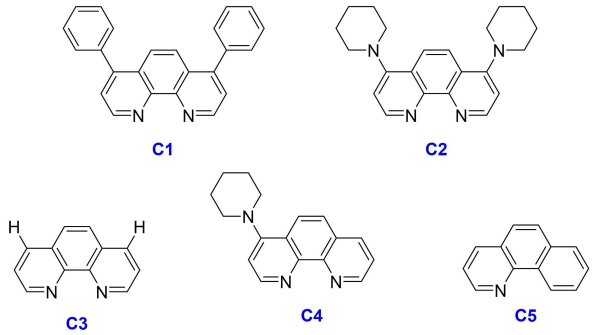

[a] All reactions were conducted with 1 (0.2 mmol) and 2 (0.1 mmol) in MTBE (0.5 M).
[b] Yield of isolated 3 averaged over two to three runs.
[c] Diastereoselectivity (α:β) was determined by ^{1}H NMR.

role of the second nitrogen atom on the phenanthroline to the C1-hydrogen of the sugar moiety observed by NMR study (Figure 2). In our NMR study (Figures 1 and 2), DTBMP was used as acid scavenger of HBr to avoid the side-product previously observed with use of IBO.[10] Further exploration revealed that replacement of IBO with DTBMP as acid scavenger resulted in improved α-1,2-*cis* diastereoselectivity while maintaining comparable yield (entries 2 and 4 vs 1 and 3). We rationalized that utilizing DTBMP as acid scavenger would preserve bromide ion in the reaction, which further facilitating the equilibrium between the glycosyl phenanthrolinium ion intermediate and the α-glycosyl bromide (Figure 3).[10]

Reaction Scope. Based on the results obtained in Table 1 and with kinetic study, we next examined the ability of **C2** catalyst with the highly hindered D-glucose and L-rhamnose 4-hydroxyl acceptors **10**–**12** (Table 2) with electron-donating glycosyl bromide donors. For instance, coupling of **10** with a donor **1**, under the influence of **C1**, provided disaccharide **16** in 55% yield with moderate α-selectivity (α:β = 7:1, entry 1).[8] This result suggests that the S_N1-S_N2 reaction paradigm is slightly shifted in the presence of the hindered alcohol **10**. Use of DTBMP as acid scavenger led slightly increase in yield (55%→71%) and α-selectivity (7:1→10:1) in favor of **16**. Use of **C2** as the catalyst maintained the yield and selectivity (entry 1). Although the α/β selectivity of the resulting disaccharide **16** was determined by the standard ^{1}H NMR analysis, it can be challenging due to the overlap of the anomeric protons with the benzyl protons. This issue was overcome by introducing the 4-fluorobenzyl group onto C6 of glucoside acceptor **11**, wherein the α/β selectivity of the resulting disaccharide **17** was determined using ^{19}F NMR (entry 2).[22] The ArF-resonance of α-isomer **17** appeared at $\delta_F = -115.07$ ppm while β-isomer counterpart appeared at $\delta_F = -114.49$ ppm. Although coupling of **11** with donor **1**, under the influence of **C1** result in slightly higher yield compared to the **C2**, diastereoselectivity significantly improved (10:1→20:1, entry 2) using **C2** catalyst. Notably, when we coupled galactosyl bromide **7** to C4-hydroxyl **11** under the influence of both **C1** and **C2**, the yield of the coupling product **18** increased while α-selectivity remained excellent compared to glucosyl bromide **1** (entry 3). Again, **C2** catalyst is more α-selective than **C1** catalyst.

Next, we examined the glycosylation reaction of challenging C4-hydroxyl rhamnose acceptor **12** with L-fucosyl bromide **8** (Table 2, entry 4). Under the influence of **C1**, the coupling product **19** (entry 4) were obtained in moderate α-selectivity (α:β = 5:1). Diastereoselectivity of **19** significantly improved (5:1→12:1) using **C2**. An important consequence of **C2** is its effectiveness with many different coupling partners. For example, **C1**-catalyzed glycosylation of serine residue **13** with **8** provided glycoconjugate **20** with moderate α-selectivity (α:β = 6:1, entry 5). In contrast, use of **C2** in the analogous reaction substantially increased in selectivity from 6:1 to 11:1 in favor of α-1,2-*cis* glycoside **20**. We also noted that **C2** catalyst is more selective with electron-withdrawing acceptor **15** (α:β = 16:1, entry 7) than with electron-donating acceptor **14** (α:β = 8:1, entry 6). We rationalized that the less reactive nucleophile **15** allows the equilibrium of the reactive glycosyl intermediates shifts toward β-glycosyl phenanthrolinium ion (Figure 3), further enhancing the diastereoselectivity of the final product **22**. Unfortunately, the phenanthroline system proved to be less robust with the combination of highly unreactive donor **9** and highly hindered acceptor **10** (entry 8).

Next, we sought to evaluate the performance of functionally complex nucleophiles in the site-selective reaction catalyzed by **C2** catalyst (Scheme 4).[23] Dexamethasone **24**, bearing a variety of functional groups and three hydroxyls, is an anti-inflammatory

Table 2. Stereoselective Glycosylation Reactions Using **C1** and **C2** Catalysts.[a]

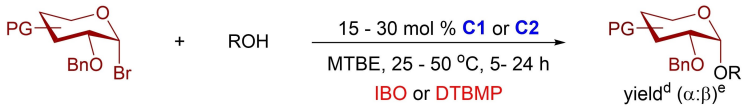

entry	donors	acceptors	proudcts	C1 Catalyst	C2 Catalyst
1	**1**	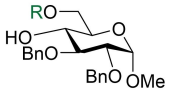 **10:** R = Bn; **11**: R = 4-F-Bn	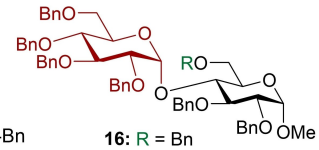 **16:** R = Bn	IBO, 50 °C[b] 55% (α:β = 7:1) DTBMP, 50 °C[b] 71% (α:β = 10:1)	DTBMP, 50 °C[b] 54% (α:β = 10:1)
2	**1**	**11**	**17:** R = 4-F-Bn	DTBMP, 50 °C[b] 79% (α:β = 10:1)	DTBMP, 50 °C[b] 72% (α:β = 20:1)
3	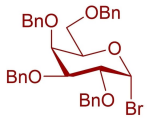 **7**	**11**	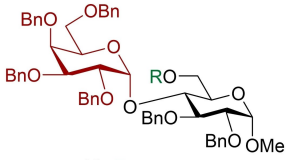 **18:** R = 4-F-Bn	DTBMP, 50 °C[b] 92% (α:β = 11:1)	DTBMP, 50 °C[b] 90% (α:β = 13:1)
4	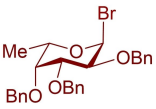 **8**	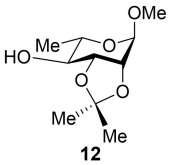 **12**	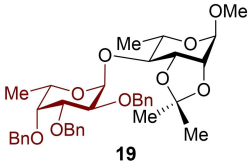 **19**	IBO, 50 °C[c] 58% (α:β = 4:1) DTBMP, 25 °C[c] 37% (α:β = 5:1)	DTBMP, 25 °C[c] 46% (α:β = 12:1)
5	**8**	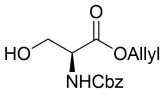 **13**	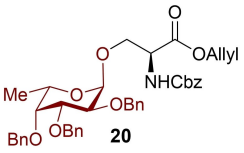 **20**	IBO, 25 °C[b] 80% (α:β = 6:1) DTBMP, 25 °C[b] 85% (α:β = 6:1)	DTBMP, 25 °C[b] 99% (α:β = 11:1)
6	**1**	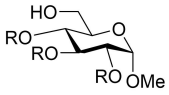 **14** (R = Bn)	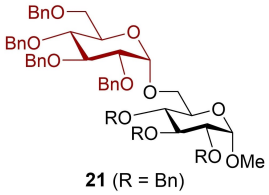 **21** (R = Bn)		DTBMP, 25 °C[b,f] 90% (α:β = 8:1)
7	**1**	**15** (R = Bz)	**22** (R = Bz)		DTBMP, 25 °C[b,f] 88% (α:β = 16:1)
8	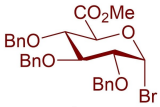 **9**	**10**	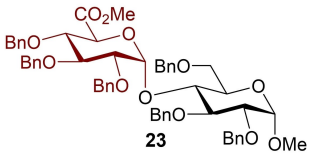 **23**	IBO, 50 °C[c] 11% (α:β = 5:1) DTBMP, 50 °C[c] 17% (α:β = 17:1)	DTBMP, 50 °C[c] 27% (α:β > 20:1)

[a] All reactions were conducted with glycosyl bromide (0.2 mmol) and alcohol acceptor (0.1 mmol) in MTBE (0.5 M).
[b] Reaction complete at 24 h.
[c] Reaction was allowed to stir for 48 h.
[d] Yield of isolated products averaged over two to three runs.
[e] The α/β selectivity was determined either by ^{1}H NMR or by ^{19}F NMR.
[f] Reaction was run in CH_2Cl_2.

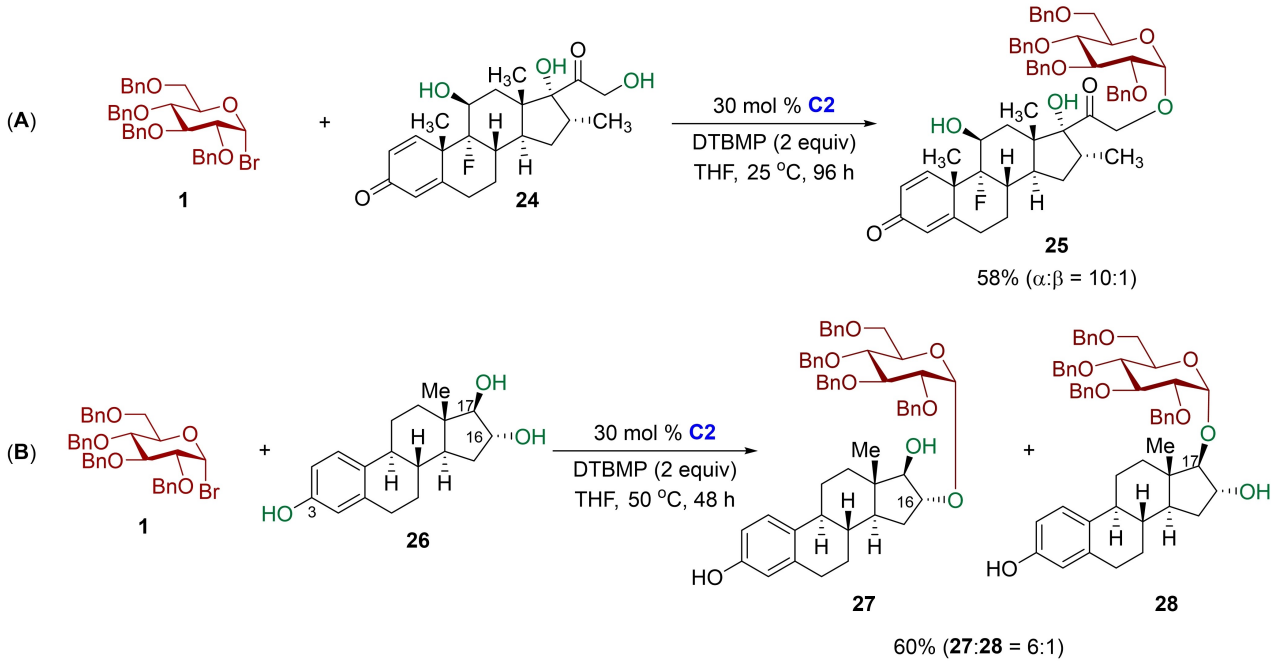

Scheme 4. C2-Catalyzed Site-Selective Couplings of Functionally Diverse Substrates.

and immunosuppressive corticosteroid that has been used as the drug to treat severe COVID-19 patients.[24] Although there are three potential coupling sites in dexamethasone **24**, we hypothesized that a primary hydroxyl would be the preferred site. As expected, a 58% yield of the coupling product **25** was obtained with high selectivity (α:β = 10:1) and complete site-selectivity (Scheme 4A) when **C2** was employed in the reaction. Estriol **26**, bearing three hydroxyl groups at the C3, C16, and C17 positions, was then evaluated to furnish a 6:1 mixture of regioisomers **27** and **28** (Scheme 4B) in 60% yield with almost exclusive α-selectivity. In this reaction, the C16-hydroxyl is the preferred site for glycosylation forming **27** as a major product while the more hindered C17-hydroxyl site afforded minor product **28**. More importantly, the glycosylation at the C3-phenol site was not observed in the reaction, suggesting that that an alkyl hydroxyl can be site-selectively coupled in the present of a phenol nucleophile.

Chemoselective Glycosylation. In typical approaches to the synthesis of oligosaccharides, an electrophile is glycosylated with a nucleophile in the presence of external reagents or catalysts, and the resulting disaccharide undergoes additional steps for selective anomeric deprotection followed by installation of an anomeric latent leaving group after each coupling. In principles, **C2**-controlled approach could streamline the needs for anomeric deprotection and protecting group manipulations. We envisioned that a glycosyl bromide is activated by **C2** catalyst and subsequently coupled to a carbohydrate acceptor incorporated with an alkyl hydroxyl as well as an unprotected C1-hemiacetal functionality. Ideally, the primary or secondary alkyl hydroxyl would be chemoselectively glycosylated in the presence of the C1-hemiacetal. The resulting hemiacetal-terminated disaccharide can be directly converted into a glycosyl donor or is directly used as an electrophilic donor for another coupling iteration to selectively furnish the corresponding oligosaccharide. The key issue of chemoselectivity relies on the nucleophilic difference between the alkyl hydroxyls and the C1-hydroxyl within the carbohydrate acceptor itself. Due to the inductive effect of the pyranose ring oxygen, we hypothesized that an alkyl hydroxyl is likely to be more nucleophilic than a C1-hydroxyl. The influence of donor reactivity in chemoselective glycosylation reactions has been well-documented.[25] In contrast, our chemoselective glycosylation strategy focuses on the effect of acceptor nucleophilicity, which has been underdeveloped.[27]

We aimed to address these limitations by examining the efficacy of the **C2** catalyst to promote both stereo- and chemoselective glycosylation of carbohydrate diol acceptors. Furthermore, the concept of chemoselectivity can only be realized under the conditions that do not promote oligomerization of the carbohydrate diol. To validate the critical questions of stereo- and chemoselectivity, a coupling of 1,6-diol acceptor **29** with glycosyl bromide **1** was examined under the influence of **C2** (Table 3, entry 1).

We selected diol **29** to test the feasibility of the chemoselective concept as it incorporates a relatively

Table 3. **C2**-Catalyzed Chemoselective Glycosylation.[a]

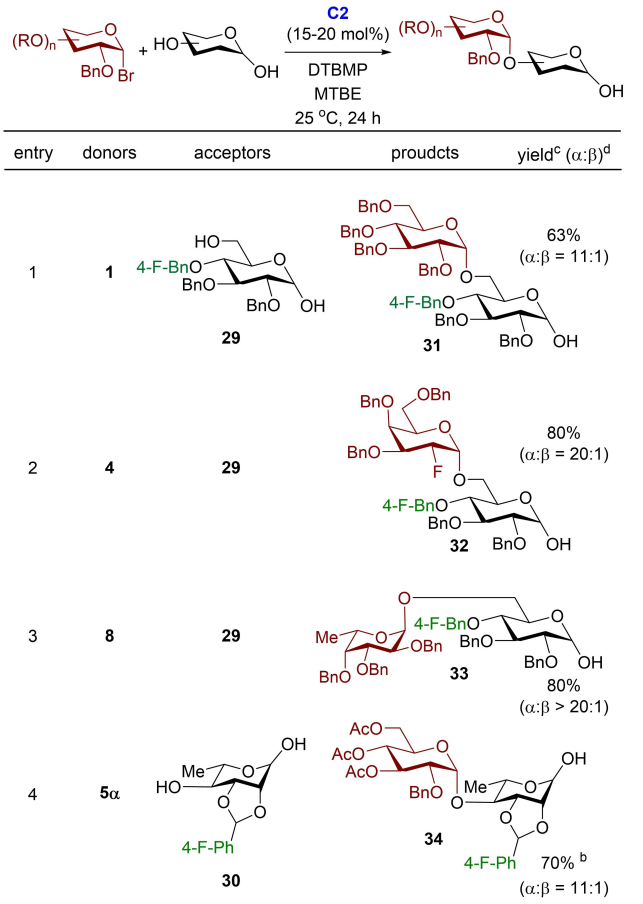

[a] Reactions were conducted with glycosyl bromide (0.1 mmol) and diol acceptor (0.15 mmol) in MTBE (0.5 M).
[b] Reactions were conducted with 0.3 mmol diol acceptor.
[c] Yield of isolated products averaged over two to three runs.
[d] The α/β selectivity was determined either by 1H NMR or by 19F NMR.

unhindered C6-hydroxyl as the preferred site for glycosylation. Under optimal **C2**-catalyzed conditions, the desired hemiacetal-terminated disaccharide **31** was obtained in 63% yield with excellent stereoselectivity (α:β = 11:1) and complete chemoselectivity (entry 1). Importantly, self-coupling of diol acceptor **29** to form 1,1'-linked disaccharide was not observed in the reaction. We next examined fluorinated diol acceptor **29** in glycosylations with glycosyl bromide donors **4** and **8** (entries 2 and 3), the yields and α-selectivities of these reactions were excellent (80%, α:β ≥ 20:1). Notably, these glycosylation reactions proceeded with complete chemoselectivity.

Having demonstrated that the **C2**-catalyzed chemoselective couplings of primary alcohols within carbohydrate acceptors in the presence of free C1-hydroxyls, this chemistry was further explored with secondary alcohol within carbohydrate acceptor **30** (Table 3, entries 4). The diol **30** incorporates a highly hindered C4-hydroxyl as the preferred site for the coupling to take place. To our excitement, coupling of diol **30** with electron-withdrawing glycosyl bromide **5α** donor (entry 4) also proceeded with complete chemoselectivity to afford the 1,4-linked disaccharide **34** in 70% yield with high diastereoselectivity (α:β = 11:1). More importantly, self-coupling of 1,4-diol acceptor **30** to form 1,1-linked disaccharide was also not observed in the reactions.

Orthogonal Glycosylation. The concept of orthogonal glycosylation focuses on the relative reactivities of glycosyl donors, which can be modulated by protecting groups and anomeric latent leaving group. Successful glycosylations require the anomeric leaving group of each carbohydrate coupling partner to be chemically distinct and activated by different reagents.[28] The orthogonal glycosylation strategy streamlines the need for anomeric derivatization steps as the coupling products are directly used as glycosyl donors for subsequent glycosylation. This concept has been applied to the synthesis of complex oligosaccharides.[28] However, subtle changes to the structures of carbohydrate coupling partners and protecting groups could impact glycosylation selectivity and reactivity. In addition, the process is not catalytic. We sought to assess the efficiency of **C2** catalyst to promote the couplings of carbohydrate coupling partners possessing chemically distinct anomeric leaving groups. Thioglycoside **35** and glycosyl bromide **1** was used in the first combination (Scheme 5A) as their anomeric leaving groups can be activated by different sets of external reagent and catalyst. The **C2** catalyzed orthogonal reaction was evaluated under optimized standard conditions with use of dichloromethane as a solvent because thioglycoside **35** was partially soluble in MTBE. The disaccharide product **36** (Scheme 5A) was obtained in 89% yield with good α-selectivity (α:β = 8:1). Similarly, the

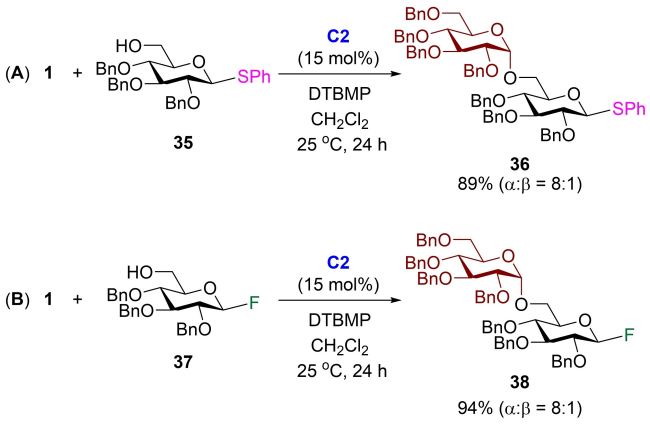

Scheme 5. **C2**-Catalyzed Orthogonal Glycosylations.

combination of glycosyl fluoride **37** and glycosyl bromide **1** under the influence of **C2** catalyst provided disaccharide **38** (Scheme 5B) in good yield and selectivity.

Conclusion

A systematic mechanistic investigation of the 4,7-dipiperidine substituted phenanthroline **C2** catalyzed-stereoselective α-1,2-cis glycosylation reaction with α-glycosyl bromide donor was performed employing variable temperature NMR (^{1}H, COSY, and ROESY) experiments. In this respect, NMR studies have showed that activation of deuterated tetrabenzyl glucosyl bromide with **C2** catalyst can readily form the two phenanthrolinium ion intermediates: the β-isomer adopts a $^4C_1$ chair conformation while the α-isomer adopts a $B_{2,5}$ boat conformation. These two glycosyl intermediates exist in a ratio of 2:1 favoring the $^4C_1$ chair-like β-phenanthrolinium ion. The ^{1}H and COSY NMR studies indicate that there is an intramolecular hydrogen bonding between the anomeric C1- proton of the carbohydrate moiety and the second pyridine nitrogen of phenanthroline framework for the two glycosyl phenanthrolinium ion intermediates. The coupling is governed by Curtin-Hammett principles and proceeds through the more reactive $^4C_1$ chair-like β-phenanthrolinium ion. The α-anomeric selectivity is rationalized by a model in which nucleophilic attack takes place from the α-face of the β-covalent glycosyl phenanthrolinium ion intermediate. Kinetic study suggested that the phenanthroline-catalyzed reaction operates by associative mechanisms.

Experimental Section

To a 10 mL oven-dried Schlenk flask, added alcohol **2** (0.1 mmol, 1.0 equiv.), catalyst (0.015 mmol, 15 mol%), acid scavenger (IBO or DTBMP, 0.2 mmol, 2.0 equiv.), then transferred glycosyl bromide **1** (0.2 mmol, 2 equiv.) with MTBE (0.2 mL). The resulting solution was stirred at 25 °C for 5 h, then directly subjected to Biotage Isolera One purification system to give **3** as a colorless syrup.

Acknowledgements

This research was supported by the National Institutes of Health (R01GM098285). The authors would like to thank Prof. Schlegel and Dr. Schaugaard at Wayne State University for their helpful advice and assistance in DFT calculations. The authors also would like to thank the Wayne State University Chemistry Lumigen Center for instrument assistance.

References

[1] A. Varki, *Glycobiology* **1993**, *3*, 97–130.

[2] a) W. L. Leng, H. Yao, J. X. He, X. W. Liu, *Acc. Chem. Res.* **2018**, *51*, 628–639; b) M. M. Nielsen, C. M. Pedersen, *Chem. Rev.* **2018**, *118*, 8285–8358; c) X. H. Li, J. L. Zhu, *Eur. J. Org. Chem.* **2016**, *2016*, 4724–4767; S. S. Nigudkar, A. V. Demchenko, *Chem. Sci.* **2015**, *6*, 2687–2704; d) M. J. McKay, H. M. Nguyen, *ACS Catal.* **2012**, *2*, 1563–1595; e) X. M. Zhu, R. R. Schmidt, *Angew. Chem. Int. Ed.* **2009**, *48*, 1900–1934; *Angew. Chem.* **2009**, *121*, 1932–1967.

[3] a) J. Dinkelaar, L. J. van den Bos, W. F. Hogendorf, G. Lodder, H. S. Overkleeft, J. D. Codee, G. A. van der Marel, *Chem. Eur. J.* **2008**, *14*, 9400–9411; b) Y. Q. Geng, A. Kumar, H. M. Faidallah, H. A. Albar, I. A. Mhkalid, R. R. Schmidt, *Angew. Chem. Int. Ed.* **2013**, *52*, 10089–10092; *Angew. Chem.* **2013**, *125*, 10273–10277; c) J.-H. Kim, H. Yang, J. Park, G.-J. Boons, *J. Am. Chem. Soc.* **2005**, *127*, 12090–12097; d) S. R. Lu, Y. H. Lai, J. H. Chen, C. Y. Liu, K. K. Mong, *Angew. Chem. Int. Ed.* **2011**, *50*, 7315–7320; *Angew. Chem.* **2011**, *123*, 7453–7458; e) S. R. Sanapala, S. S. Kulkarni, *J. Am. Chem. Soc.* **2016**, *138*, 4938–4947; f) L. M. Wang, H. S. Overkleeft, G. A. van der Marel, J. D. C. Codee, *J. Am. Chem. Soc.* **2018**, *140*, 4632–4638; g) J. P. Yasomanee, A. V. Demchenko, *J. Am. Chem. Soc.* **2012**, *134*, 20097–20102; h) Q. J. Zhang, E. R. van Rijssel, M. T. C. Walvoort, H. S. Overkleeft, G. A. van der Marel, J. D. C. Codee, *Angew. Chem. Int. Ed.* **2015**, *54*, 7670–7673; *Angew. Chem.* **2015**, *127*, 7780–7783; i) Y. X. Zhang, S. H. Zhou, X. H. Wang, H. Zhang, Z. W. Guo, J. Gao, *Org. Chem. Front.* **2019**, *6*, 762–772; j) D. Crich, *Acc. Chem. Res.* **2010**, *43*, 1144–1153; k) M. Huang, G. E. Garrett, N. Birlirakis, L. Bohe, D. A. Pratt, D. Crich, *Nat. Chem.* **2012**, *4*, 663–667; l) Y. Ito, T. Ogawa, *Angew. Chem. Int. Ed.* **1994**, *33*, 1765–1767; *Angew. Chem.* **1994**, *106*, 1843–1845; m) H. Nguyen, D. Y. Zhu, X. H. Li, J. L. Zhu, *Angew. Chem. Int. Ed.* **2016**, *55*, 4767–4771; *Angew. Chem.* **2016**, *128*, 4845–4849; n) Y. Okada, N. Asakura, M. Bando, Y. Ashikaga, H. Yamada, *J. Am. Chem. Soc.* **2012**, *134*, 6940–6943; o) L. J. van den Bos, J. Dinkelaar, H. S. Overkleeft, G. A. van der Marel, *J. Am. Chem. Soc.* **2006**, *128*, 13066–13067.

[4] a) T. Kimura, T. Eto, D. Takahashi, K. Toshima, *Org. Lett.* **2016**, *18*, 3190–3193; b) Q. H. Li, S. M. Levi, E. N. Jacobsen, *J. Am. Chem. Soc.* **2020**, *142*, 11865–11872; c) E. A. Mensah, F. Yu, H. M. Nguyen, *J. Am. Chem. Soc.* **2010**, *132*, 14288–14302; d) Y. Park, K. C. Harper, N. Kuhl, E. E. Kwan, R. Y. Liu, E. N. Jacobsen, *Science* **2017**, *355*, 162–166; e) P. Peng, R. R. Schmidt, *J. Am. Chem. Soc.* **2015**, *137*, 12653–12659; f) G. C. Sati, J. L. Martin, Y. S. Xu, T. Malakar, P. M. Zimmerman, J. Montgomery, *J. Am. Chem. Soc.* **2020**, *142*, 7235–7242; g) M. Shadrick, Y. Singh, A. V. Demchenko, *J. Org. Chem.* **2020**, *85*, 15936–15944; h) E. T. Sletten, Y. J. Tu, H. B. Schlegel, H. M. Nguyen, *ACS Catal.* **2019**, *9*,

2110–2123; i) L. F. Sun, X. W. Wu, D. C. Xiong, X. S. Ye, *Angew. Chem. Int. Ed.* **2016**, *55*, 8041–8044; *Angew. Chem.* **2016**, *128*, 8173–8176; j) F. Yu, J. L. Dickson, R. S. Loka, H. F. Xu, R. C. R. Schaugaard, E. H. R. Schlegel, L. Luo, E. Nguyen, *ACS Catal.* **2020**, *10*, 5990–6001; k) L. L. Lairson, B. Henrissat, G. J. Davies, S. G. Withers, *Annu. Rev. Biochem.* **2008**, *77*, 521–555; l) R. M. Schmaltz, S. R. Hanson, C. H. Wong, *Chem. Rev.* **2011**, *111*, 4259–4307.

[5] a) G. C. Fu, *Acc. Chem. Res.* **2000**, *33*, 412–420; b) S. France, D. J. Guerin, S. J. Miller, T. Lectka, *Chem. Rev.* **2003**, *103*, 2985–3012.

[6] S. J. Miller, *Acc. Chem. Res.* **2004**, *37*, 601–610.

[7] a) R. U. Lemieux, A. R. Morgan, *J. Am. Chem. Soc.* **1963**, *85*, 1889–1890; b) R. U. Lemieux, A. R. Morgan, *Can. J. Chem.* **1965**, *43*, 2205–2213.

[8] F. Yu, J. Y. Li, P. M. DeMent, Y. J. Tu, H. B. Schlegel, H. M. Nguyen, *Angew. Chem. Int. Ed.* **2019**, *58*, 6957–6961; *Angew. Chem.* **2019**, *131*, 7031–7035.

[9] a) A. Bencini, V. Lippolis, *Coord. Chem. Rev.* **2010**, *254*, 2096–2180; b) K. E. Erkkila, D. T. Odom, J. K. Barton, *Chem. Rev.* **1999**, *99*, 2777–2795.

[10] P. M. DeMent, C. Liu, J. Wakpal, R. N. Schaugaard, H. B. Schlegel, H. M. Nguyen, *ACS Catal.* **2021**, *11*, 2108–2120.

[11] a) P. J. Stephens, F. J. Devlin, C. F. Chabalowski, M. J. Frisch, *J. Phys. Chem.* **1994**, *98*, 11623–11627; b) A. D. Becke, *J. Chem. Phys.* **1993**, *98*, 5648–5652; c) C. T. Lee, W. T. Yang, R. G. Parr, *Phys. Rev. B* **1988**, *37*, 785–789; d) A. D. Becke, *Phys. Rev. A* **1988**, *38*, 3098–3100; e) S. H. Vosko, L. Wilk, M. Nusair, *Can. J. Phys.* **1980**, *58*, 1200–1211; f) M. M. Francl, W. J. Pietro, W. J. Hehre, J. S. Binkley, M. S. Gordon, D. J. Defrees, J. A. Pople, *J. Chem. Phys.* **1982**, *77*, 3654–3665; g) M. S. Gordon, *Chem. Phys. Lett.* **1980**, *76*, 163–168; h) P. C. Hariharan, J. A. Pople, *Mol. Phys.* **1974**, *27*, 209–214; i) Pc. Harihara, J. A. Pople, *Theor. Chim. Acta* **1973**, *28*, 213–222; j) W. J. Hehre, R. Ditchfield, J. A. Pople, *J. Chem. Phys.* **1972**, *56*, 2257–2261; k) R. Ditchfield, W. J. Hehre, J. A. Pople, *J. Chem. Phys.* **1971**, *54*, 724–728.

[12] A. V. Marenich, C. J. Cramer, D. G. Truhlar, *J. Phys. Chem. B* **2009**, *113*, 6378–6396.

[13] a) S. Grimme, J. Antony, S. Ehrlich, H. Krieg, *J. Chem. Phys.* **2010**, *132*, 154104; b) E. R. Johnson, A. D. Becke, *J. Chem. Phys.* **2006**, *124*, 024101.

[14] M. J. Frisch, G. W. Trucks, H. B. Schlegel, G. E. Scuseria, M. A. Robb, J. R. Cheeseman, G. Scalmani, V. Barone, G. A. Petersson, H. Nakatsuji, X. Li, M. Caricato, A. V. Marenich, J. Bloino, B. G. Janesko, R. Gomperts, B. Mennucci, H. P. Hratchian, J. V. Ortiz, A. F. Izmaylov, J. L. Sonnenberg, Williams, F. Ding, F. Lipparini, F. Egidi, J. Goings, B. Peng, A. Petrone, T. Henderson, D. Ranasinghe, V. G. Zakrzewski, J. Gao, N. Rega, G. Zheng, W. Liang, M. Hada, M. Ehara, K. Toyota, R. Fukuda, J. Hasegawa, M. Ishida, T. Nakajima, Y. Honda, O. Kitao, H. Nakai, T. Vreven, K. Throssell, J. A. Montgomery Jr., J. E. Peralta, F. Ogliaro, M. J. Bearpark, J. J. Heyd, E. N. Brothers, K. N. Kudin, V. N. Staroverov, T. A. Keith, R. Kobayashi, J. Normand, K. Raghavachari, A. P. Rendell, J. C. Burant, S. S. Iyengar, J. Tomasi, M. Cossi, J. M. Millam, M. Klene, C. Adamo, R. Cammi, J. W. Ochterski, R. L. Martin, K. Morokuma, O. Farkas, J. B. Foresman, D. J. Fox, Wallingford, CT, **2013**.

[15] R. U. Lemieux, *Pure Appl. Chem.* **1971**, *27*, 527–548.

[16] A. J. Dingley, F. Cordier, S. Grzesiek, *Concepts Magn. Reson.* **2001**, *13*, 103–127.

[17] E. Skorupowa, B. Dmochowska, J. Madaj, F. Kasprzykowski, J. Sokołowski, A. Wiśniewski, *J. Carbohydr. Chem.* **1998**, *17*, 49–59.

[18] B. A. Garcia, D. Y. Gin, *J. Am. Chem. Soc.* **2000**, *122*, 4269–4279.

[19] a) N. Sorgenfrei, J. Hioe, J. Greindl, K. Rothermel, F. Morana, N. Lokesh, R. M. Gschwind, *J. Am. Chem. Soc.* **2016**, *138*, 16345–16354; b) F. Ibba, G. Pupo, A. L. Thompson, J. M. Brown, T. D. W. Claridge, V. Gouverneur, *J. Am. Chem. Soc.* **2020**, *142*, 19731–19744.

[20] T. I. Mizan, P. E. Savage, R. M. Ziff, *J. Phys. Chem.* **1996**, *100*, 403–408.

[21] R. U. Lemieux, K. B. Hendriks, R. V. Stick, K. James, *J. Am. Chem. Soc.* **1975**, *97*, 4056–4062.

[22] C. Saunders, M. B. Khaled, J. D. Weaver, D. J. Tantillo, *J. Org. Chem.* **2018**, *83*, 3220–3225.

[23] S. A. Blaszczyk, T. C. Homan, W. P. Tang, *Carbohydr. Res.* **2019**, *471*, 64–77.

[24] a) R. M. Johnson, J. M. Vinetz, *Br. Med. J.* **2020**, *370*; b) T. Lammers, A. M. Sofias, R. van der Meel, R. Schiffelers, G. Storm, F. Tacke, S. Koschmieder, T. H. Brummendorf, F. Kiessling, J. M. Metselaar, *Nat. Nanotechnol.* **2020**, *15*, 622–624.

[25] B. Fraser-Reid, J. C. López, in *Reactivity Tuning in Oligosaccharide Assembly* (Eds.: B. Fraser-Reid, J. Cristóbal López), Springer Berlin Heidelberg, Berlin, Heidelberg, **2011**, pp. 1–29.

[26] S. van der Vorm, T. Hansen, J. M. A. van Hengst, H. S. Overkleeft, G. A. van der Marel, J. D. C. Codee, *Chem. Soc. Rev.* **2019**, *48*, 4688–4706.

[27] H. M. Nguyen, J. L. Poole, D. Y. Gin, *Angew. Chem. Int. Ed.* **2001**, *40*, 414–417; *Angew. Chem.* **2001**, *113*, 428–431.

[28] a) O. Kanie, Y. Ito, T. Ogawa, *J. Am. Chem. Soc.* **1994**, *116*, 12073–12074; b) Y. Ito, O. Kanie, T. Ogawa, *Angew. Chem. Int. Ed.* **1996**, *35*, 2510–2512; *Angew. Chem.* **1996**, *108*, 2691–2693; c) O. Kanie, I. Ohtsuka, T. Ako, S. Daikoku, Y. Kame, R. Kato, *Angew. Chem. Int. Ed.* **2006**, *45*, 3851–3854; *Angew. Chem.* **2006**, *118*, 3935–3938.

RESEARCH ARTICLE

A Mechanistic Probe into 1,2-*cis* Glycoside Formation Catalyzed by Phenanthroline and Further Expansion of Scope

Adv. Synth. Catal. **2021**, *363*, 1 – 14

J. Li, H. M. Nguyen*